Geophysical Research Letters

RESEARCH LETTER
10.1029/2023GL104726

Potential Non-Linearities in the High Latitude Circulation and Ozone Response to Stratospheric Aerosol Injection

Ewa M. Bednarz[1,2,3], Daniele Visioni[4,5], Amy H. Butler[2], Ben Kravitz[6,7], Douglas G. MacMartin[3], and Simone Tilmes[5]

[1]Cooperative Institute for Research in Environmental Sciences (CIRES), University of Colorado Boulder, Boulder, CO, USA, [2]NOAA Chemical Sciences Laboratory (NOAA CSL), Boulder, CO, USA, [3]Sibley School of Mechanical and Aerospace Engineering, Cornell University, Ithaca, NY, USA, [4]Department of Earth and Atmospheric Sciences, Cornell University, Ithaca, NY, USA, [5]Atmospheric Chemistry Observations and Modelling (ACOM), National Center for Atmospheric Research (NCAR), Boulder, CO, USA, [6]Department of Earth and Atmospheric Sciences, Indiana University, Bloomington, IN, USA, [7]Atmospheric Sciences and Global Change Division, Pacific Northwest National Laboratory, Richland, WA, USA

Abstract The impacts of Stratospheric Aerosol Injection (SAI) on the atmosphere and surface climate depend on when and where the sulfate aerosol precursors are injected, as well as on how much surface cooling is to be achieved. We use a set of CESM2(WACCM6) SAI simulations achieving three different levels of global mean surface cooling and demonstrate that unlike some direct surface climate impacts driven by the reflection of solar radiation by sulfate aerosols, the SAI-induced changes in the high latitude circulation and ozone are more complex and could be non-linear. This manifests in our simulations by disproportionally larger Antarctic springtime ozone loss, significantly larger intra-ensemble spread of the Arctic stratospheric jet and ozone responses, and non-linear impacts on the extratropical modes of surface climate variability under the strongest-cooling SAI scenario compared to the weakest one. These potential non-linearities may add to uncertainties in projections of regional surface impacts under SAI.

Plain Language Summary The injection of reflective aerosols, or their precursors, into the lower stratosphere (Stratospheric Aerosol Injection, SAI) has been proposed as a temporary measure to offset some of the adverse impacts of climate change whilst atmospheric concentrations of greenhouses are being stabilized and, ultimately, reduced. The impacts of SAI on the atmosphere and surface climate would depend on when and where the sulfate aerosol precursors are injected, as well as on how much surface cooling is to be achieved. Here we analyze SAI impacts on stratospheric climate and ozone in a set of Earth system model simulations under varying magnitudes of the SAI-induced global mean cooling. We demonstrate that unlike some of the direct surface climate impacts from the reflection of solar radiation by sulfate aerosols, the SAI-induced changes in stratospheric circulation, chemistry and climate are more complex, with the model simulations pointing toward more non-linear behavior of the high latitude circulation and ozone under higher SAI scenarios. These potential non-linearities may add to uncertainties in projections of regional surface impacts under SAI.

Key Points:

- Impacts of Stratospheric Aerosol Injection (SAI) depend on how much surface cooling is to be achieved
- High latitude circulation, ozone and modes of extratropical variability can vary non-linearly with the SAI-induced global surface cooling
- These potential non-linearities may add to uncertainties in projections of regional surface impacts under SAI

Supporting Information:

Supporting Information may be found in the online version of this article.

Correspondence to:

E. M. Bednarz,
ewa.bednarz@noaa.gov

Citation:

Bednarz, E. M., Visioni, D., Butler, A. H., Kravitz, B., MacMartin, D. G., & Tilmes, S. (2023). Potential non-linearities in the high latitude circulation and ozone response to stratospheric aerosol injection. *Geophysical Research Letters*, *50*, e2023GL104726. https://doi.org/10.1029/2023GL104726

Received 30 MAY 2023
Accepted 8 OCT 2023

Author Contributions:

Conceptualization: Ewa M. Bednarz, Daniele Visioni, Amy H. Butler, Ben Kravitz, Douglas G. MacMartin
Data curation: Daniele Visioni
Formal analysis: Ewa M. Bednarz, Daniele Visioni
Funding acquisition: Amy H. Butler, Douglas G. MacMartin
Investigation: Ewa M. Bednarz
Methodology: Ewa M. Bednarz, Daniele Visioni, Amy H. Butler, Ben Kravitz, Douglas G. MacMartin
Validation: Amy H. Butler
Visualization: Ewa M. Bednarz

1. Introduction

The injection of reflective aerosols, or their precursors, into the lower stratosphere (Stratospheric Aerosol Injection, SAI) has been proposed as a temporary measure to offset some of the adverse impacts of climate change whilst atmospheric concentrations of greenhouses are being stabilized and, ultimately, reduced. Research in support of informed decision making for potential future SAI requires a detailed assessment of the effectiveness and efficiency of SAI as well as the associated side-effects. The latter include the warming in the tropical lower stratosphere from the absorption of radiation by sulfate aerosols, which can then impact the large-scale Brewer Dobson Circulation (BDC) and zonal winds, driving changes in both transport of stratospheric ozone and the mid and high latitude surface climate via stratosphere-troposphere coupling (Banerjee et al., 2021; Bednarz et al., 2022; Ferraro et al., 2015; Jones et al., 2022; McCusker et al., 2015; Tilmes et al., 2021, 2022). In addition, the activation of atmospheric halogens on aerosol surfaces can accelerate halogen-catalyzed ozone depletion in the lower stratosphere and, thus, slow down the ongoing recovery of stratospheric ozone layer to its pre-1980 levels (Tilmes et al., 2021, 2022).

The effectiveness of SAI in reducing surface temperatures and mitigating regional climate change will depend on where and when the aerosol precursors are injected (Bednarz et al., 2023a, 2023b; Visioni et al., 2023a;

Writing – original draft: Ewa M. Bednarz
Writing – review & editing: Ewa M. Bednarz, Daniele Visioni, Amy H. Butler, Ben Kravitz, Douglas G. MacMartin, Simone Tilmes

Zhang et al., 2023). In addition, the effectiveness of parallel GHG emission reductions will determine the overall magnitude of SAI needed to maintain or cool the temperatures to a desired level, and the resulting SAI impacts will thus also depend on this desired temperature target (MacMartin et al., 2022; Visioni et al., 2023b). Visioni et al. (2023b) analyzed some of the surface climate responses in a set of SAI simulations using the same injection strategy (i.e., the same location of SO_2 injections) but achieving different levels of global mean surface cooling (though different total magnitudes of SAI), and showed that many of the resulting changes scale broadly linearly with the amount of SAI-induced cooling.

Though the direct radiative changes at the surface behave quasi linearly with the amount of SAI, the behavior of the stratosphere-troposphere coupled circulation has been shown to be non-linear or regime-like in character in response to external forcings, both idealized thermal forcings and climate change (Charney & Drazin, 1961; Manzini et al., 2018; Walz et al., 2023; Wang et al., 2012), and thus harder to predict. Similarly, in the stratosphere the concentrations of chemical tracers like ozone are driven by a range of chemical and dynamical processes, the relative contribution of which could change under SAI. Here we analyze the SAI impacts on stratospheric climate and ozone under varying magnitudes of global mean cooling. We demonstrate that while the tropical stratospheric changes behave largely linearly, the resulting high latitude dynamical responses to SAI are more complex and could vary non-linearly with increasing magnitudes of SAI. These in turn could lead to non-linear impacts on high-latitude climate and ozone that may add to uncertainties in projections of some regional surface impacts under SAI.

2. Methods

We use the CESM2(WACCM6) earth system model (Danabasoglu et al., 2020; Gettelman et al., 2019) with interactive modal aerosol microphysics (MAM4, Liu et al., 2016) and interactive middle atmosphere chemistry (Davis et al., 2023). The horizontal resolution is 1.25° longitude by 0.9° latitude, with 70 vertical levels in hybrid-pressure coordinates up to ∼140 km. The simulations used are introduced in MacMartin et al. (2022) and described in detail in Visioni et al. (2023b). The Coupled Model Intercomparison Project Phase 6 (CMIP6) Shared Socioeconomic Pathway SSP2-4.5 experiment is chosen as a background emission scenario. In all SAI simulations SO_2 is injected at 21.5 km at four off-equatorial latitudes—30°S, 15°S, 15°N, 30°N—using a feedback algorithm that controls for the global mean surface temperature as well as its large scale interhemispheric and equator-to-pole gradients.

We use three SAI scenarios, each consisting of three ensemble members, all continuously injecting SO_2 over 2035–2069. "SAI1.5" maintains the above three temperature objectives at the levels corresponding to 1.5°C above preindustrial conditions (here defined as the 2020–2039 mean of the CESM2 SSP2-4.5 simulation, see MacMartin et al., 2022). "SAI1.0" and "SAI0.5" are similar to SAI1.5 but aim to achieve more surface cooling—global mean surface temperatures of 1.0°C and 0.5°C above preindustrial conditions, respectively—by injecting more SO_2. Averaged over the last 20 years of simulations, these simulations require 8.6, 17.0, and 25.6 Tg-SO_2/yr to achieve this, respectively. Unless stated otherwise, we analyze the last 20 years of the simulations (2050–2069) and compare them against the same period of the control SSP2-4.5 simulation.

3. Changes in Tropical Stratospheric Climate

The introduction of sulfate aerosols into the stratosphere and the resulting scattering of a portion of incoming solar radiation reduces tropical tropospheric temperatures, with the strongest reduction, by design, found in SAI0.5 and the smallest in SAI1.5 (Figure 1a). In the lower stratosphere, the absorption of some of the outgoing terrestrial and incoming solar radiation by sulfate increases local temperatures. The magnitude of this effect is in tight linear relationship with the global mean surface cooling in each of the SAI simulation, with $R^2 = 0.95$ for the goodness of fit of the individual ensemble members and $R^2 = 1.00$ for the fit to the ensemble means (Figure 1e).

The SAI-induced lower stratospheric warming drives changes in the large-scale circulation, decelerating upwelling in the upper troposphere lower stratosphere (UTLS) region and, thus, the shallow branch of the BDC, and accelerating the deep branch (Figure 1b). Changes in the large-scale transport modulate stratospheric distribution of chemical tracers, most importantly ozone. In the tropics (Figure 1d), this increases ozone in the tropical lower stratosphere (from reduced input of ozone-poor tropospheric air), decreases ozone at ∼30 hPa (from enhanced input of lower stratospheric air with lower ozone concentrations) and increases ozone above it at ∼10 hPa (from enhanced input of middle stratospheric air where ozone concentrations maximize). In addition, SAI-induced enhancement of N_2O_5 hydrolysis on aerosol surfaces removes active nitrogen species from the middle stratosphere

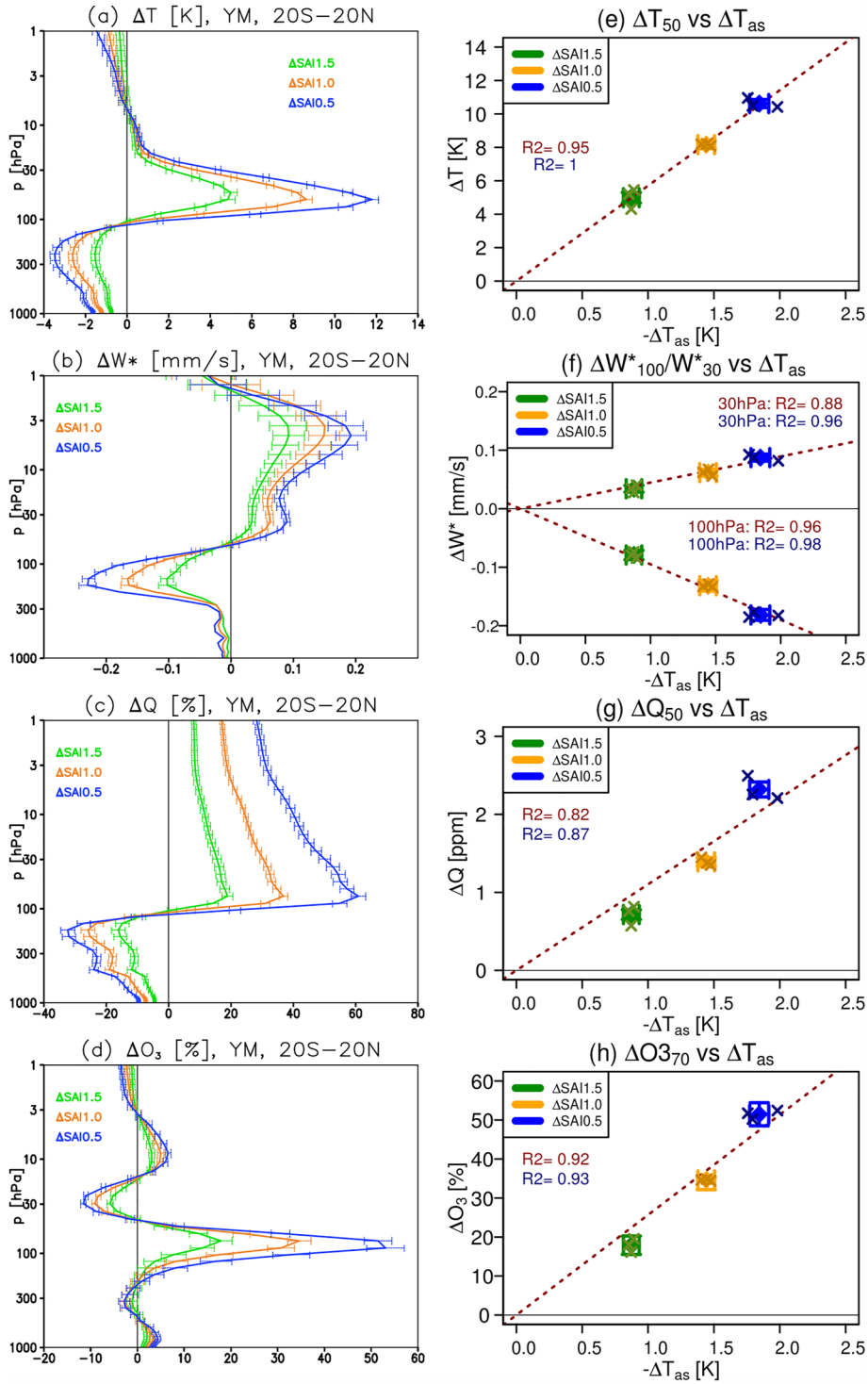

Figure 1. Yearly mean 20°S–20°N changes in (a, e) temperatures, (b, f) TEM vertical velocity, (c, g) water vapor and (d, h) ozone compared to SSP2-4.5. Left: ensemble mean response versus altitude (errorbars: ±2 standard errors of the difference in means). Right: SAI responses at a given altitude versus global mean surface cooling. Diamonds and whiskers: ensemble mean response ±2 standard error; crosses: responses in the individual ensemble members (compared to the SSP2-4.5 ensemble mean). Values of R^2 shown in red and blue correspond to the values calculated for the single ensemble members and the ensemble means, respectively.

(Bednarz et al., 2023b; Tilmes et al., 2021), thereby contributing to the increase in ozone levels around ~10 hPa. Climatologically, the absorption of solar radiation by ozone constitutes the dominant source of heat in the stratosphere and, thus, any changes in its concentration act to further modulate stratospheric temperatures. A tight correlation between SAI-induced changes in tropical lower stratospheric temperatures, ozone and transport was shown to hold also in a multi-model context (Bednarz et al., 2023a). Finally, the SAI-induced warming around the cold point tropical tropopause allows more water vapor to enter the stratosphere (Figure 1c), and this acts to offset some of the direct surface cooling as water vapor traps a portion of the outgoing terrestrial radiation (Bednarz et al., 2023b). Increased stratospheric water vapor also modulates the rates of chemical ozone loss, as well as provides additional stratospheric cooling.

Overall, the magnitudes of these tropical responses scale largely linearly with the magnitude of SAI. Small deviations from the linear relationship emerge for changes in lower stratospheric water vapor (Figure 1g) and ozone (Figure 1h), that is, for which the strong vertical gradients in the SAI-induced changes in temperatures and upwelling near the tropopause can play an important role.

4. High Latitude Dynamical Response

4.1. Stratosphere

The anomalous enhancement of the meridional temperature gradients as the result of the SAI-induced warming in the tropical lower stratosphere drives strengthening of the stratospheric jets in both hemispheres, and the magnitude of the response increases with the magnitude of SO_2 injection (Figures 2a–2c). In the Southern Hemisphere (SH) during austral winter (Figure 2e), where the very strong climatological jet prohibits much planetary wave propagation and, thus, any changes are mainly radiatively driven via the thermal wind relationship, a strong linear relationship ($R^2 = 0.94$ for the fit to the ensemble means of SAI1.5, SAI1.0 and SAI0.5) is found between the magnitude of the SH jet strengthening and the global mean surface cooling. However, in spring (SON, Figure 2g), when interactions with both planetary waves and with the SAI-induced ozone depletion within the polar vortex (Section 5) can occur, a more non-linear relationship emerges: the jet strengthening in the largest SAI scenario (SAI0.5) is disproportionally larger than that inferred for SAI1.0 and SAI1.5 (9, 4 ,and 2 m/s, respectively). For the Northern Hemisphere (NH) during winter (DJF, Figure 2d) the apparent non-linearity is even stronger: the NH jet strengthening simulated in SAI0.5 is also disproportionally larger than that in SAI1.0 and SAI1.5 (8 m/s, 4 m/s and 3 m/s, respectively), and is also characterized by a much larger spread in the zonal wind responses simulated across the individual ensemble members (blue crosses) than it is the case for either SAI1.0 and SAI1.5.

Non-linearity of the NH polar vortex response has been previously found in response to increased CO_2 forcing (Manzini et al., 2018) and to idealized heating in a dry dynamical model (Walz et al., 2023; Wang et al., 2012), and may be related to non-linearities in tropospheric wave generation that arise from SAI-induced changes in sea ice (Kretschmer et al., 2020) or surface temperatures, or to regime-like behavior in the stratospheric planetary wave guide related to subtropical wind changes (Walz et al., 2023).

4.2. Northern Hemisphere Troposphere

Through wave-mean flow interactions, extratropical stratospheric wind changes can propagate down to the troposphere and affect surface climate (Baldwin & Dunkerton, 2001; Thompson & Wallace, 2000); in the NH this coupling maximizes in winter. Under the strongest SAI0.5 scenario, the NH stratospheric westerly wind response propagates down to the surface in the form of sea-level pressure changes projecting on the positive phase of the North Atlantic Oscillation (NAO) (Figure 3f); the positive NAO-like response is diagnosed also from each individual ensemble member of SAI0.5 (Figure S1 in Supporting Information S1). This drives a dynamically induced warming over northern Eurasia (evident when the simulations are compared against past periods with the same global mean surface temperature, Figure S2c in Supporting Information S1), which acts to offset the large-scale SAI-induced cooling from the reflection of incoming solar radiation (Figures S2e and S2h in Supporting Information S1). In contrast, no significant NAO-like sea-level pressure response is found in the two smaller SAI scenarios (SAI1.0 and SAI1.5. Figures 3d and 3e).

We note that in the Northern Pacific sector, on the other hand, all SAI scenarios show increased sea-level pressures compared to SSP2-4.5 that project on the weakening of the Aleutian low, the magnitude of which increases with the magnitude of SAI. Unlike the top-down dynamical contribution from the stratosphere, however, the response is likely driven predominantly by the SAI-induced tropospheric cooling, as it is opposite in sign to the

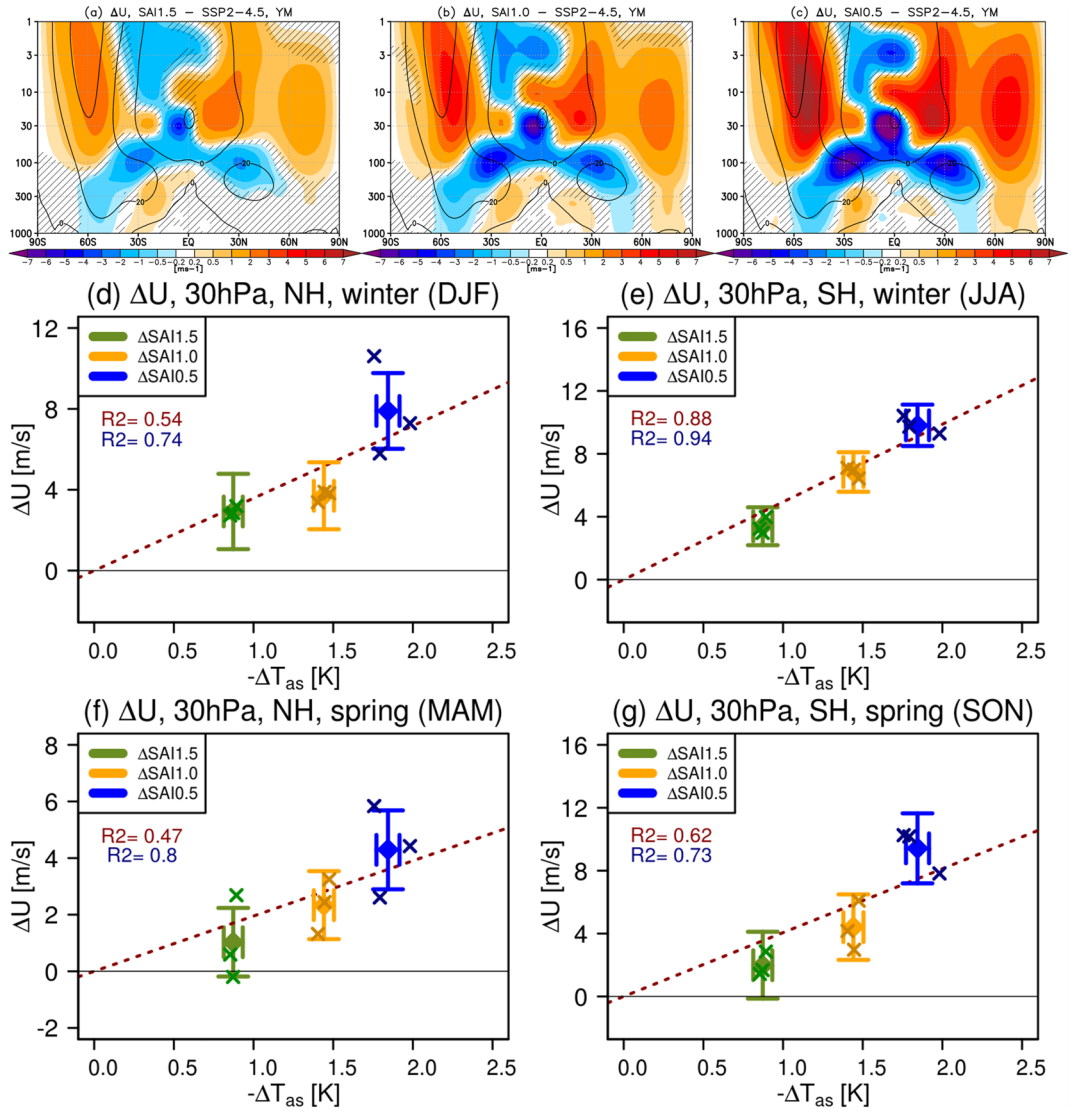

Figure 2. (a–c) Shading: yearly mean changes in zonal winds compared to SSP2-4.5. Contours: values in SSP2-4.5. Hatching denotes response is not statistically significant (±2 standard error of the difference in means). (d–g) Changes in the strength of the NH (60°N, d,f) and SH (50°S, e,g) polar vortex at 30 hPa in winter (d,e) and spring (f,g) versus global mean surface cooling compared to SSP2-4.5. Diamonds and whiskers, crosses and R^2 as in Figure 1.

response to GHG in SSP2-4.5 alone (Figure S3b in Supporting Information S1); as such it largely disappears if the SAI scenarios are compared against past periods with the same global mean surface temperatures (Figure S4 in Supporting Information S1).

The strength of the stratosphere-troposphere coupling can be assessed by correlating the changes in the NH stratospheric jet with the NAO index for each of the ensemble members and scenarios. Following our earlier work (Bednarz et al., 2023b) we calculate the model NAO index as the difference in sea-level pressure between the Atlantic mid-latitudes (280°E–360°E, 30°N–60°N) and the Arctic polar cap (70°N–90°N, all longitudes). Over the 20-year mean period analyzed here, we find a strong relationship between the strength of the stratospheric winds and surface NAO responses for the three ensemble members of the strongest SAI scenario (SAI0.5), with stronger stratospheric westerly anomalies associated with more positive NAO values (blue points in Figure 3g). In contrast, no such relationship can be inferred for the responses in the individual ensemble members of the two smaller SAI scenarios (SAI1.0 and SAI1.5). An analysis of temporal evolution of the responses reveals that the apparent non-linearity emerges toward the end of the simulations (Figure S5 in Supporting Information S1), where the injection rates are highest.

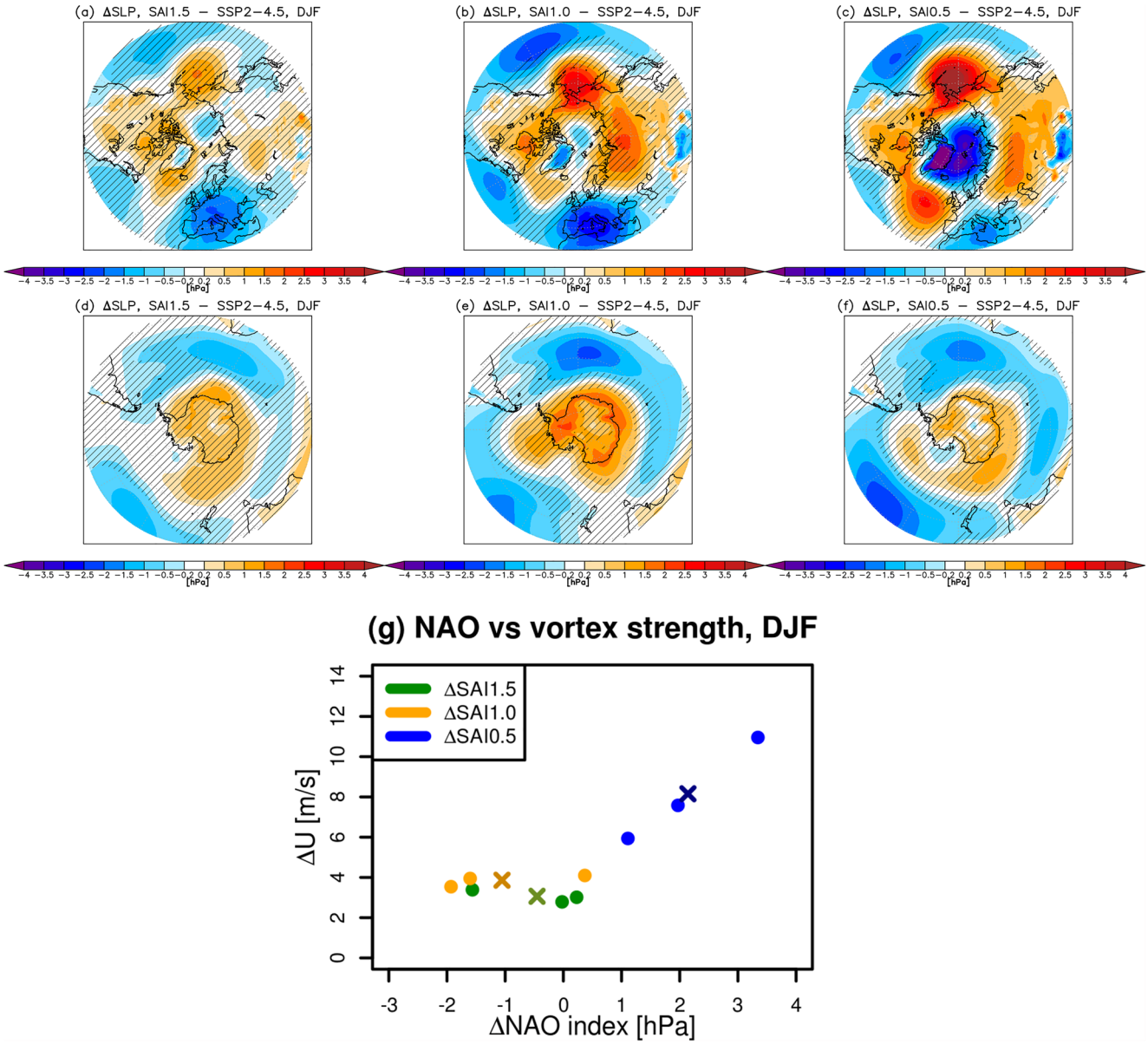

Figure 3. DJF sea-level pressure changes (a–c) northward of 30°N, and (d–f) southward of 30°S compared to SSP2-4.5. Hatching as in Figure 2. (g): Correlation between the DJF changes in the strength of the NH stratospheric polar vortex (60°N, 30 hPa) and in the NAO sea-level pressure index. Points: responses in each ensemble member; crosses: ensemble mean responses.

Such apparent nonlinearity in the NH surface responses may result from the non-linearity in the stratospheric jet response itself (Section 4.1), or from non-linearities in the tropospheric circulation or sea ice and sea surface temperatures that either discourage or promote the canonical downward coupling from the stratosphere on the NAO (Kolstad et al., 2022). Another possibility is that the enhanced stratosphere-troposphere coupling under the largest SAI scenario arises because the response is only for that case strong enough to emerge from the background natural variability, which is particularly high in the NH winter (Bittner et al., 2016; DallaSanta & Polvani, 2022).

4.3. Southern Hemisphere Troposphere

Anomalies in the SH stratospheric jet can also propagate down to the troposphere and affect the SH surface climate; such stratospheric influence tends to maximize in austral spring and summer (SON and DJF). We find that the SAI-induced westerly stratospheric anomalies do not propagate down to the surface in any of the SAI

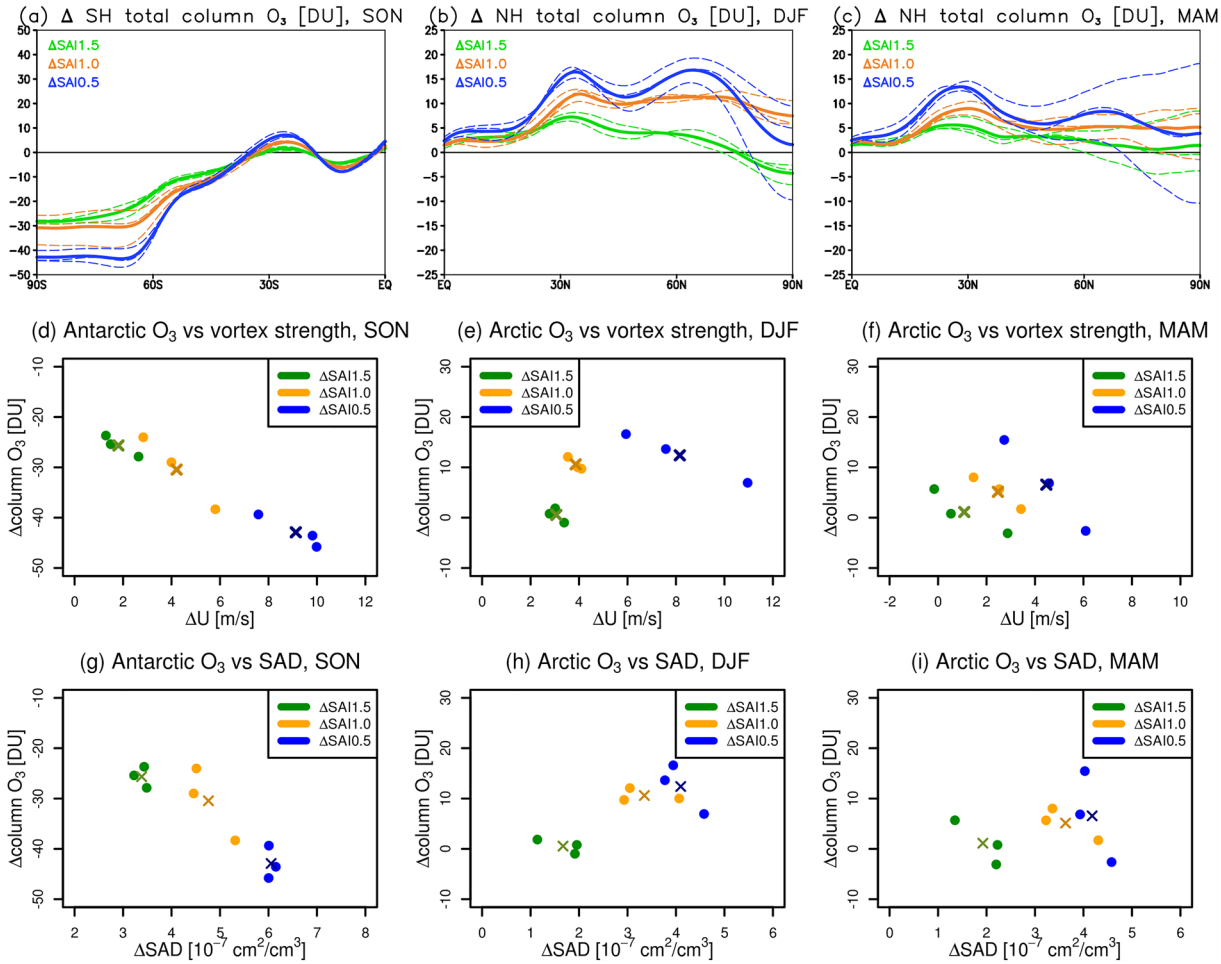

Figure 4. Impacts on the Arctic and Antarctic ozone. (a–c) Seasonal mean changes in total column ozone in (left) SON in the SH, (middle) DJF in the NH and (right) MAM in the NH compared to SSP2-4.5. Thick lines: ensemble mean responses; dashed lines: responses in each ensemble member (compared to the SSP2-4.5 ensemble mean). (d–i) Correlation between seasonal mean changes in (d–f) polar (65°–90°) ozone and stratospheric vortex strength (as in Figures 2d–2g), and between changes in (g–i) polar ozone and polar SAD at 170 hPa. Points and crosses as in Figure 3g.

simulations (Figure 3h–3j). This is the case even for the strongest SAI0.5 scenario that shows disproportionally larger stratospheric jet perturbation in spring than the smaller SAI1.0 and SAI1.5 (Figure 3j). We would expect a strengthened SH stratospheric jet in austral spring to lead to a later than average seasonal transition of the polar vortex and an associated shift toward the positive phase of the Southern Annular Mode (SAM) in austral summer (Thompson et al., 2005). Instead, all SAI scenarios give rise to a pattern of sea-level pressure changes projecting onto the negative phase of SAM, inferred both from DJF (Figures 3h–3j) and yearly mean (Figure S6 in Supporting Information S1) data, with no clear linear relationship between the strength of the SAM-like sea-level pressure pattern and the SAI magnitude. This suggests that factors other than the magnitude of the injection, especially the meridional distribution of sulfate in the stratosphere (Bednarz et al., 2022), are more important in determining the SH high latitude tropospheric and surface response to SAI.

5. Impacts on Arctic and Antarctic Ozone

5.1. Antarctic Ozone

In austral spring, the SH high latitude ozone columns decrease under all three SAI scenarios compared to the same period of SSP2-4.5 because of the enhancement of heterogeneous halogen activation on sulfate and the resulting catalytic stratospheric ozone depletion inside the Antarctic polar vortex (Figure 4a). In addition, the strengthening of the polar vortex inhibits mixing with the more ozone-rich mid-latitude air, thereby further reducing polar

ozone levels. We find similar Antarctic (65°S–90°S) ozone losses of 26 DU (=9%) and 30 DU (=11%) for the two lower SAI scenarios, SAI1.5 and SAI1.0, respectively. In contrast, a significantly higher Antarctic ozone loss of 43 DU (=15%) is found for the largest SAI0.5 scenario.

A tight linear relationship is found between the polar ozone column reductions and the strengthening of the Antarctic polar vortex across the simulations (Figure 4d), as well as between the ozone changes and the increased sulfate surface area densities (SAD, Figure 4g). A stronger and colder polar vortex under more aggressive SAI scenario accelerates halogen activation and chemical ozone loss as well as delays final vortex break; both factors enhance Antarctic ozone reduction under SAI. Conversely, the enhanced ozone depletion under higher sulfate SAD cools the polar stratosphere and, thus, strengthens the stratospheric zonal winds (Keeble et al., 2014). The strong linear relationship between these quantities under varying SAI levels demonstrates how the same processes operate under all three SAI scenarios. The cause of the apparent non-linearity and thus the significantly higher magnitude of the Antarctic springtime ozone loss in SAI0.5 compared to SAI1.0 and SAI1.5 is thus dynamical in origin, in line with the significantly larger strengthening of the polar vortex in SAI0.5 than the other two scenarios (Figure 2g).

5.2. Arctic Ozone

Unlike in the SH, the NH ozone columns largely increase under SAI during boreal winter and spring (Figures 4b and 4c) due to the SAI-induced changes in the BDC and the resulting ozone transport (Section 3; see also Tilmes et al., 2022; Bednarz et al., 2023b). Owing to the Arctic vortex being climatologically weaker and more variable than its SH counterpart, the chemical impacts from the SAI-induced enhancement of the heterogenous halogen processing on the elevated SAD are generally smaller. Consistently, SAI1.5 shows increased NH winter total ozone columns in the mid- and high latitudes up to ~75°N, with a small total column ozone decrease poleward. For SAI1.0, the total column ozone changes are positive everywhere and larger in magnitude than for SAI1.5; this indicates that the impact of SAI on the BDC dominates over chemically and dynamically driven ozone reductions inside the polar vortex in this scenario. In spring, ozone columns increase throughout the NH in the ensemble mean for both SAI1.5 and SAI0.5, albeit with larger variability between the individual ensemble members than during winter (dashed lines in Figures 4b and 4c).

An interesting picture emerges for the largest SAI0.5 scenario: whilst ozone columns increase in winter in the ensemble mean throughout the NH, the magnitude of the response is sharply reduced in the Arctic region, with substantially larger variability between the individual ensemble members. In fact, one ensemble member of SAI0.5 shows the strongest decrease in Arctic ozone at the pole from all the SAI simulations and members. The large intra-ensemble variability continues into spring, with individual members of SAI0.5 showing both the most positive and the most negative Arctic column ozone perturbations. The large springtime ozone variability extends to the mid-latitudes, as anomalies in polar ozone mix-in with the mid-latitude air following the vortex break-up. The contrastingly different ozone behavior in SAI0.5 is concurrent with the strongest and more non-linear high latitude dynamical response identified above (Sections 4.1 and 4.2). Owing to the interplay of various dynamical and chemical processes in the Arctic, with its opposing impacts on total ozone column, the previously identified linear relationship between changes in the Antarctic ozone, polar vortex and sulfate SAD (Figures 4d and 4g) is generally not found in the Arctic during winter (Figures 4e and 4h). The inverse relationship between changes in polar ozone and vortex strength is only apparent under the strongest SAI0.5 scenario, facilitated by the much larger variability between the ensemble members.

Recent studies highlighted the role of dynamical and chemical ozone reductions inside the Arctic polar vortex in modulating the northern polar jet dynamics (Friedel et al., 2022a, 2022b; Kult-Herdin et al., 2023). However, it was also demonstrated that this ozone feedback, as manifested by the inverse relationship between polar ozone and jet strength, is only found under the present-day (i.e., high) levels of ozone-depleting substances where ozone variability is larger (Kult-Herdin et al., 2023). It is possible that the same occurs under SAI, that is, the feedback from interactive ozone in our runs only starts to play a significant role in contributing to the polar vortex behavior under the strongest SAI0.5 scenario, where the sulfate SAD and, thus, chemical ozone depletion is largest.

In spring, the inverse relationship between polar ozone and vortex strength (Figure 4f) emerges for each individual SAI scenario. This indicates that the differences in springtime ozone responses across the different SAI scenarios (Figure 4c) are driven predominantly by the SAI-induced changes in the BDC, whereas the intra-ensemble spread in each scenario is associated more linearly with chemical-dynamical feedbacks.

6. Summary and Discussion

The impacts of SAI on the atmosphere and surface climate would depend on when and where the sulfate aerosol precursors are injected, as well as on how much surface cooling is to be achieved. We have demonstrated that unlike some of the direct surface climate impacts from the reflection of solar radiation by sulfate aerosols (Visioni et al., 2023b), the SAI-induced changes in stratospheric circulation, chemistry and climate are more complex, with the model simulations pointing toward more non-linear behavior of the high latitude circulation and ozone under higher SAI scenarios.

In particular, the SAI-induced changes in the tropical stratospheric temperatures, upwelling, water vapor and ozone are found to scale roughly linearly with the magnitude of global mean cooling in CESM2 under the multi-objective SAI strategy used. A significantly more non-linear behavior is found for the associated extra-tropical stratospheric zonal wind responses, in particular in seasons when the wave-mean flow coupling plays an important role. In those cases, a disproportionally stronger westerly jet anomaly is simulated for the largest SAI scenario (SAI0.5) compared to the more modest ones. In the SH, this is associated with markedly stronger (~50%) Antarctic springtime ozone depletion in SAI0.5. In the NH, the non-linearity manifests in part as the significantly larger intra-ensemble spread of the SAI-induced changes in the stratospheric jet strength and Arctic ozone columns in SAI0.5. The scenario also gave rise to much stronger NH stratosphere-troposphere coupling, facilitating the propagation of the stratospheric westerly response down to the surface in the form of the positive North Atlantic Oscillation, which was otherwise not reproduced for the two smaller SAI scenarios. Regarding impacts on the Southern Annular Mode, the analogous propagation of the SH polar vortex strengthening to the troposphere is not found under any SAI scenario; this points to other factors like the meridional distribution of sulfate in the stratosphere (and thus the location of the injection; as discussed in Bednarz et al., 2022) being more important in determining the SAI impacts in the region.

The results highlight the complexity of the impacts of SAI on stratospheric climate, high latitude circulation and stratospheric ozone, including the complex interplay of various chemical, radiative and dynamical processes. Dynamical mechanisms for abrupt regime changes driving the dynamical responses to thermal perturbations were previously found in idealized models (Walz et al., 2023; Wang et al., 2012). Whether these mechanisms apply also to more complex climate models is still not well understood, but non-linearities in the stratospheric jet response to different levels of global warming have previously been found (Manzini et al., 2018). The role of chemically driven Arctic and Antarctic ozone reductions in modulating the polar vortex behavior has also been highlighted as a potentially important feedback mechanism that is still not sufficiently understood (Friedel et al., 2022a, 2022b; Keeble et al., 2014; Kult-Herdin et al., 2023). Here evidence of such feedback was shown to be particularly strong under the largest SAI scenario, that is, when the higher stratospheric aerosol levels drive larger chemical ozone losses that can then modulate the polar vortex dynamics. Finally, though not examined in detail in this study, changes in stratospheric water vapor have also been shown to drive changes in the high latitude circulation (Maycock et al., 2013; Seabrook et al., 2023), as well as enhance catalytic ozone loss (Tilmes et al., 2021), but uncertainties remain as to the details of such responses. Since SAI-induced lower stratospheric warming also drives significant increases in stratospheric water vapor, this process constitutes an additional source of uncertainty to the overall SAI impacts in the high latitudes.

We note that our results could be model dependent. In addition, with three ensemble members per experiment, a rigorous assessment of the origin of these dynamical differences is beyond the scope of the current study. However, the apparent non-linear behavior of the high latitude circulation and ozone response to SAI merits further assessment in a multi-model framework and with larger ensembles, as part of ongoing efforts in narrowing the uncertainties in the climate response to SAI.

Data Availability Statement

Data used in this manuscript is available from Bednarz and Visioni (2023).

Acknowledgments
We would like to acknowledge high-performance computing support from Cheyenne (https://doi.org/10.5065/D6RX99HX) provided by NCAR's Computational and Information Systems Laboratory, sponsored by the National Science Foundation. Support was provided by the NOAA cooperative agreement NA22OAR4320151, NOAA Earth's Radiative Budget initiative, Atkinson Center for a Sustainability at Cornell University, and by the National Science Foundation through agreement CBET-2038246. Support for BK was provided in part by the National Science Foundation through agreement SES-1754740 and the Indiana University Environmental Resilience Institute.

References

Baldwin, M. P., & Dunkerton, T. J. (2001). Stratospheric harbingers of anomalous weather regimes. *Science*, *294*(5542), 581–584. https://doi.org/10.1126/science.1063315

Banerjee, A., Butler, A. H., Polvani, L. M., Robock, A., Simpson, I. R., & Sun, L. (2021). Robust winter warming over Eurasia under stratospheric sulfate geoengineering – The role of stratospheric dynamics. *Atmospheric Chemistry and Physics*, *21*(9), 6985–6997. https://doi.org/10.5194/acp-21-6985-2021

Bednarz, E. M., Butler, A. H., Visioni, D., Zhang, Y., Kravitz, B., & MacMartin, D. G. (2023b). *Injection strategy – A driver of atmospheric circulation and ozone response to stratospheric aerosol geoengineering*. EGUsphere (preprint). https://doi.org/10.5194/egusphere-2023-495

Bednarz, E. M., & Visioni, D. (2023). Data from: 'Potential non-linearities in the high latitude circulation and ozone response to stratospheric aerosol injection' [Dataset]. Zenodo. https://doi.org/10.5281/zenodo.7976364

Bednarz, E. M., Visioni, D., Kravitz, B., Jones, A., Haywood, J. M., Richter, J., et al. (2023a). Climate response to off-equatorial stratospheric sulfur injections in three Earth system models – Part 2: Stratospheric and free-tropospheric response. *Atmospheric Chemistry and Physics*, *23*(1), 687–709. https://doi.org/10.5194/acp-23-687-2023

Bednarz, E. M., Visioni, D., Richter, J. H., Butler, A. H., & MacMartin, D. G. (2022). Impact of the latitude of stratospheric aerosol injection on the Southern Annular Mode. *Geophysical Research Letters*, *49*(19), e2022GL100353. https://doi.org/10.1029/2022GL100353

Bittner, M., Schmidt, H., Timmreck, C., & Sienz, F. (2016). Using a large ensemble of simulations to assess the Northern Hemisphere stratospheric dynamical response to tropical volcanic eruptions and its uncertainty. *Geophysical Research Letters*, *43*(17), 9324–9332. https://doi.org/10.1002/2016GL070587

Charney, J. G., & Drazin, P. G. (1961). Propagation of planetary-scale disturbances from lower into upper atmosphere. *Journal of Geophysical Research*, *66*(1), 83–109. https://doi.org/10.1029/JZ066i001p00083

DallaSanta, K., & Polvani, L. M. (2022). Volcanic stratospheric injections up to 160 Tg(S) yield a Eurasian winter warming indistinguishable from internal variability. *Atmospheric Chemistry and Physics*, *22*(13), 8843–8862. https://doi.org/10.5194/acp-22-8843-2022

Danabasoglu, G., Lamarque, J.-F., Bacmeister, J., Bailey, D. A., DuVivier, A. K., Edwards, J., et al. (2020). The community Earth system model version 2 (CESM2). *Journal of Advances in Modeling Earth Systems*, *12*, e2019MS001916. https://doi.org/10.1029/2019MS001916

Davis, N. A., Visioni, D., Garcia, R. R., Kinnison, D. E., Marsh, D. R., Mills, M. J., et al. (2023). Climate, variability, and climate sensitivity of "Middle atmosphere" chemistry configurations of the community Earth system model version 2, whole atmosphere community climate model version 6 (CESM2(WACCM6)). *Journal of Advances in Modeling Earth Systems*, *15*(9), e2022MS003579. https://doi.org/10.1029/2022MS003579

Ferraro, A. J., Charlton-Perez, A. J., & Highwood, E. J. (2015). Stratospheric dynamics and midlatitude jets under geoengineering with space mirrors and sulfate and titania aerosols. *Journal of Geophysical Research: Atmospheres*, *120*(2), 414–429. https://doi.org/10.1002/2014jd022734

Friedel, M., Chiodo, G., Stenke, A., Domeisen, D., Fueglistaler, S., Anet, J., & Peter, T. (2022b). Springtime arctic ozone depletion forces Northern Hemisphere climate anomalies. *Nature Geoscience*, *15*(7), 541–547. https://doi.org/10.1038/s41561-022-00974-7

Friedel, M., Chiodo, G., Stenke, A., Domeisen, D., & Peter, T. (2022a). Effects of Arctic ozone on the stratospheric spring onset and its surface impact. *Atmospheric Chemistry and Physics*, *22*(21), 13997–14017. https://doi.org/10.5194/acp-22-13997-2022

Gettelman, A., Mills, M. J., Kinnison, D. E., Garcia, R. R., Smith, A. K., Marsh, D. R., et al. (2019). The whole atmosphere community climate model version 6 (WACCM6). *Journal of Geophysical Research: Atmospheres*, *124*(23), 12380–12403. https://doi.org/10.1029/2019JD030943

Jones, A., Haywood, J. M., Scaife, A. A., Boucher, O., Henry, M., Kravitz, B., et al. (2022). The impact of stratospheric aerosol intervention on the North Atlantic and Quasi-Biennial Oscillations in the geoengineering model intercomparison project (GeoMIP) G6sulfur experiment. *Atmospheric Chemistry and Physics*, *22*(5), 2999–3016. https://doi.org/10.5194/acp-22-2999-2022

Keeble, J., Braesicke, P., Abraham, N. L., Roscoe, H. K., & Pyle, J. A. (2014). The impact of polar stratospheric ozone loss on Southern Hemisphere stratospheric circulation and climate. *Atmospheric Chemistry and Physics*, *14*(24), 13705–13717. https://doi.org/10.5194/acp-14-13705-2014

Kolstad, E. W., Lee, S. H., Butler, A. H., Domeisen, D. I. V., & Wulff, C. O. (2022). Diverse surface signatures of stratospheric polar vortex anomalies. *Journal of Geophysical Research: Atmospheres*, *127*(20), e2022JD037422. https://doi.org/10.1029/2022JD037422

Kretschmer, M., Zappa, G., & Shepherd, T. G. (2020). The role of Barents–Kara sea ice loss in projected polar vortex changes. *Weather and Climate Dynamics*, *1*(2), 715–730. https://doi.org/10.5194/wcd-1-715-2020

Kult-Herdin, J., Sukhodolov, T., Chiodo, G., Checa-Garcia, R., & Rieder, H. (2023). The impact of different CO2 and ODS levels on the mean state and variability of the springtime Arctic stratosphere. *Environmental Research Letters*, *18*(2), 024032. https://doi.org/10.1088/1748-9326/acb0e6

Liu, X., Ma, P.-L., Wang, H., Tilmes, S., Singh, B., Easter, R. C., et al. (2016). Description and evaluation of a new four-mode version of the modal aerosol module (MAM4) within version 5.3 of the community atmosphere model. *Geoscientific Model Development*, *9*(2), 505–522. https://doi.org/10.5194/gmd-9-505-2016

MacMartin, D. G., Visioni, D., Kravitz, B., Richter, J., Felgenhauer, T., Lee, W. R., et al. (2022). Scenarios for modeling solar radiation modification. *Proceedings of the National Academy of Sciences of the United States of America*, *119*(33). https://doi.org/10.1073/pnas.2202230119

Manzini, E., Karpechko, A. Y., & Kornblueh, L. (2018). Nonlinear response of the stratosphere and the North Atlantic-European climate to global warming. *Geophysical Research Letters*, *45*(9), 4255–4263. https://doi.org/10.1029/2018GL077826

Maycock, A. C., Joshi, M. M., Shine, K. P., & Scaife, A. A. (2013). The circulation response to idealized changes in stratospheric water vapor. *Journal of Climate*, *26*(2), 545–561. https://doi.org/10.1175/JCLI-D-12-00155.1

McCusker, K. E., Battisti, D. S., & Bitz, C. M. (2015). Inability of stratospheric sulfate aerosol injections to preserve the West Antarctic Ice Sheet. *Geophysical Research Letters*, *42*(12), 4989–4997. https://doi.org/10.1002/2015gl064314

Seabrook, M., Smith, D. M., Dunstone, N. J., Eade, R., Hermanson, L., Scaife, A. A., & Hardiman, S. C. (2023). Opposite impacts of interannual and decadal Pacific variability in the extratropics. *Geophysical Research Letters*, *50*(2), e2022GL101226. https://doi.org/10.1029/2022GL101226

Thompson, D. W. J., Baldwin, M. P., & Solomon, S. (2005). Stratosphere–Troposphere coupling in the Southern Hemisphere. *Journal of the Atmospheric Sciences*, *62*(3), 708–715. https://doi.org/10.1175/JAS-3321.1

Thompson, D. W. J., & Wallace, J. M. (2000). Annular modes in the extratropical circulation. Part I: Month-to-month variability. *Journal of Climate*, *13*(5), 1000–1016. https://doi.org/10.1175/1520-0442(2000)01360;1000:amitec62;2.0.co;2

Tilmes, S., Richter, J. H., Kravitz, B., MacMartin, D. G., Glanville, A. S., Visioni, D., et al. (2021). Sensitivity of total column ozone to stratospheric sulfur injection strategies. *Geophysical Research Letters*, *48*(19), e2021GL094058. https://doi.org/10.1029/2021GL094058

Tilmes, S., Visioni, D., Jones, A., Haywood, J., Séférian, R., Nabat, P., et al. (2022). Stratospheric ozone response to sulfate aerosol and solar dimming climate interventions based on the G6 Geoengineering Model Intercomparison Project (GeoMIP) simulations. *Atmospheric Chemistry and Physics*, *22*(7), 4557–4579. https://doi.org/10.1029/2022GL094058

Visioni, D., Bednarz, E. M., Lee, W. R., Kravitz, B., Jones, A., Haywood, J. M., & MacMartin, D. G. (2023a). Climate response to off-equatorial stratospheric sulfur injections in three Earth system models – Part 1: Experimental protocols and surface changes. *Atmospheric Chemistry and Physics*, *23*(1), 663–685. https://doi.org/10.5194/acp-23-663-2023

Visioni, D., Bednarz, E. M., MacMartin, D. G., Kravitz, B., & Goddard, P. (2023b). The choice of baseline period influences the assessments of the outcomes of Stratospheric Aerosol Injection. *Earth's Future*, *11*(8), e2023EF003851. https://doi.org/10.1029/2023EF003851

Walz, R., Garny, H., & Birner, T. (2023). Stratospheric modulation of tropical upper-tropospheric warming-induced circulation changes in an idealized general circulation model. *Journal of the Atmospheric Sciences*, *80*(2), 611–631. https://doi.org/10.1175/JAS-D-21-0232.1

Wang, S., Gerber, E. P., & Polvani, L. M. (2012). Abrupt circulation responses to tropical upper-tropospheric warming in a relatively simple stratosphere-resolving AGCM. *Journal of Climate*, *25*(12), 4097–4115. https://doi.org/10.1175/JCLI-D-11-00166.1

Zhang, Y., MacMartin, D. G., Visioni, D., Bednarz, E., & Kravitz, B. (2023). *Introducing a comprehensive set of stratospheric aerosol injection strategies*. EGUsphere (preprint). https://doi.org/10.5194/egusphere-2023-117